

TURNOVER OF ROD PHOTORECEPTOR OUTER SEGMENTS

II. Membrane Addition and Loss in Relationship to Light

JOSEPH C. BESHARSE, JOE G. HOLLYFIELD, and MARY E. RAYBORN

From the Departments of Anatomy and Ophthalmology, College of Physicians and Surgeons, Columbia University, New York 10032. The present address for Dr. Hollyfield and Ms. Rayborn is the Department of Ophthalmology, Baylor College of Medicine, Houston, Texas 77030. Dr. Besharse's present address is the Department of Anatomy, School of Medicine, Emory University, Atlanta, Georgia 30322.

ABSTRACT

The rate of disk addition to rod outer segments (ROS) varies widely in *Xenopus laevis* tadpoles kept in cyclic light (12L:12D). When measured as radioactive band (^3H -band) displacement during the 2nd day after injection of [^3H]leucine, 75% of the daily increment of displacement occurred during the first 8 h of light. During the same interval, the number of open disks at the ROS base increased more than threefold. During the last 8 h of darkness, ^3H -band displacement was undetectable and the number of open disks was reduced. These observations suggest the possibility that disk addition may occur discontinuously. During the 3rd and 4th days after injection of [^3H]leucine, maximal displacement of the ^3H -band occurred later in the day than on the 2nd day, its movement no longer corresponding to the increase in open disks. This delay in ^3H -band displacement may reflect a time delay as a result of propagation of compressive stress in an elastic ROS system. Maximal disk loss from ROS as reflected in counts of phagosomes in the pigment epithelium occurred within 1 h of light exposure, and phagosome counts remained high for 4 h before declining to a low level in darkness.

Modified lighting regimes affected the daily rhythms of shedding and disk addition differently, suggesting that control mechanisms for the two processes are not directly coupled. During 3 days in darkness, disk addition was reduced 50% compared to controls (12L:12D), whereas shedding was reduced by about 40%. Although reduced in level, shedding occurred as a free-running circadian rhythm. There was no evidence of rhythmicity of disk addition in darkness. In constant light, the rate of disk addition was not different from controls, but shedding was reduced by about 80% after the 1st day. This resulted in a 21% increase in ROS length. Among animals kept on a 2.5L:21.5D cycle, the rate of disk addition was reduced by 40% while shedding was maintained near control levels, resulting in a slight decrease in ROS length. These observations indicate that normal shedding requires alternating light and darkness, and that the daily rhythm of disk addition is due primarily to daily stimulation by light.

Rod photoreceptor outer segments (ROS) are membranous structures containing a membrane-bound visual pigment (45) which is bleached in light (44). Most of the membrane lipid is in the form of a bilayer (7, 45), and the visual pigment is a glycoprotein (23) containing either retinal or 3-dehydroretinal as the chromophore (10). Isomerization of the chromophore in light leads to hyperpolarization of the plasma membrane (18, 43) and decreased synaptic activity (39, 40). The visual pigment makes up about 80% of the protein of the ROS (9, 21) and is found in both disks and plasma membrane (3, 27).

Most of the ROS membrane (Fig. 1) is arranged as a series of closed disks derived from and contained within the plasma membrane (13, 14, 36, 41). The ROS is connected to the inner segment by a cilium (41), and adjacent to the cilium a series of disks are often observed whose

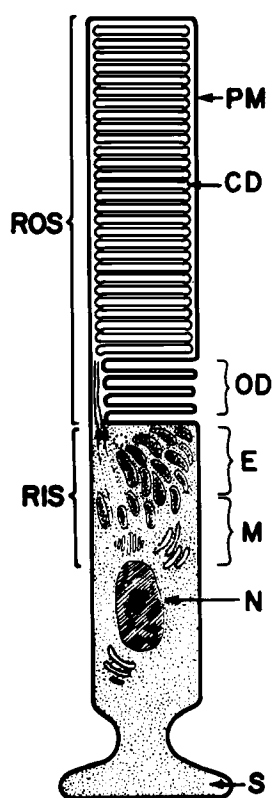


FIGURE 1 Diagram illustrating the structure of a rod photoreceptor. ROS, rod outer segment; RIS, rod inner segment; PM, plasma membrane; CD, closed disk; OD, zone of open disks; E, ellipsoid; M, myoid; N, nucleus; and S, synaptic terminal.

intradisk space is confluent with the extracellular space and whose membrane is confluent with the plasma membrane (13, 14, 30, 36). The similarity between these open disks and those formed during early differentiation of rods (36) and their proximity to the inner segment suggests that they represent sites where new disks are added to the ROS (14, 21, 36, 50).

By using autoradiography, Young (46, 49) demonstrated that ROS membranes turn over rapidly, a possibility suggested by several earlier observations (1, 16, 17, 36). When a tritiated amino acid is injected intraperitoneally, labeled protein is first detected in the myoid region of the inner segment (16, 52). From here, it is transported to the base of the ROS where an intense band of radioactivity forms in an area corresponding to the zone of open disks (46, 47, 52). Gradually, the radioactive band is displaced distally where it is lost from the ROS tip in a packet consisting of as many as 200 disks (51). These disks are phagocytized (51) and degraded by the adjacent pigment epithelium (18, 24, 26, 28, 42). Parallel extraction studies indicate that much of the radioactivity is recovered with the visual pigment (20, 21) and that the visual pigment contained in phagosomes is incapable of regeneration soon after it is phagocytized (11).

Radioactive band displacement in ROS occurs because new unlabeled disks are formed in the zone adjacent to the cilium and displace the older, labeled disks distally (46, 49, 50). Intraperitoneal injections of tritiated amino acids act effectively as pulse doses (19, 20), in that label is only transiently available. In addition, much of the radioactive protein in labeled disks is visual pigment (21). Although the visual pigment diffuses laterally within the membrane of a disk, exchange between disks does not occur (34, 38). Once radioactive visual pigment is incorporated into a disk, it is confined to that locus until the disk is lost during the shedding process at the ROS tip (50). Thus, the rate of radioactive band displacement reflects the rate of membrane (disk) addition to the ROS.

Recently, it was found that cyclic light plays a basic role in the regulation of disk loss in both rats and frogs (4, 24, 33, 32). Shedding of ROS tips occurs soon after exposure to light. In contrast, disk addition has been regarded as a continuous process which is affected by light only slightly (21, 46, 48, 50). However, our observations of increased disk addition in Ozark cave salamanders

maintained in cyclic light (5) and of a rapid recovery of ROS length after massive shedding in frog tadpoles (11) suggested that light might influence disk addition in a more fundamental way. This suggestion has been confirmed for amphibian rod photoreceptors by the use of autoradiography (6).

This paper presents autoradiographic and electron microscope observations which indicate that the rate of disk addition to ROS in *Xenopus laevis* tadpoles varies widely in cyclic light and is reduced by about 50% in darkness. In addition, experiments are described which were designed to analyze the potential interrelationship of disk addition and disk loss (shedding) in animals kept under modified lighting regimes. The results indicate that the two processes are affected differently and independently, suggesting that they are not directly coupled. Evidence is also presented that suggests the existence of an endogenous circadian rhythm of shedding.

MATERIALS AND METHODS

Animals and Treatment

Xenopus laevis tadpoles were obtained from the Amphibian Facility, University of Michigan, Ann Arbor. Before the experiments, they were kept for a minimum of 7 days at $28 \pm 0.5^\circ\text{C}$ on a diurnal cycle of 12 h of light and 12 h of darkness per day (12L:12D). Light was obtained from two 15-W incandescent bulbs with an intensity at the level of the animal containers of 200–250 lx/m². This same illumination system was used for all light treatments. Animals were kept in groups of 5–10 in 19-cm stacking dishes containing 10% Holtfreter's solution (22) and were fed hydrated nettle powder. The solution was changed and the animals were fed every 2nd or 3rd day. Animals used in experiments were at larval stages 54–56 (35). For autoradiography, tadpoles received intraperitoneal injections delivered through pipets prepared from 50- μl capillary tubes of 5 or 10 μCi of L-[(N)-4,5-³H]leucine with a spec act of 5.0 Ci/mmol (New England Nuclear, Boston, Mass.). These dosages amounted to approximately 12 or 25 $\mu\text{Ci/g}$ body wt (wet). The smaller dose was used in most experiments.

Microscopy

Two fixation procedures were used, and both were adequate for light microscopy. Within a single experiment, all eyes were treated the same way. Some eyes were fixed in 1.5% glutaraldehyde in 0.067 M cacodylate buffer (pH 7.4) containing 0.05% CaCl_2 . The second fixing solution, used for electron microscope observations, consisted of 2% paraformaldehyde and 2.5% glutaraldehyde in 0.1 M cacodylate buffer (pH 7.4) containing 0.025% CaCl_2 (24). Eyes were removed in

light or in a darkroom under dim red light (Wratten number 2 filter, 15 W bulb). Postfixation and further processing were carried out by procedures described in the preceding paper (25). Some eyes fixed by the second procedure were stained en block, immediately after osmification, in a solution of 1% uranyl magnesium acetate containing 0.17 M NaCl and 0.10 M sucrose.

Thick sections (1 μm) for immediate observation were placed on glass slides and stained with Paragon stain, Azure II, or toluidine blue. Under dim red light (Wratten number 2 filter), glass slides with unstained sections for autoradiography were dipped in Kodak nuclear track emulsion (NTB-2) diluted 1:1 with distilled water and maintained at 40°C . Autoradiographs were exposed, developed, and stained by procedures described in the preceding paper (25). Optimum exposure periods for different experiments ranged from 8 to 14 days. Ultrastructural observations were made on thin sections (silver to gray) on parlodion-coated single-slot or 200-mesh grids. Sections were stained with uranyl acetate and lead citrate and observed with a Siemens Elmiskop 1A at 80 kV.

Analysis of Autoradiographs

The object of our autoradiographic analysis was to measure displacement of a radioactive band in ROS under different experimental conditions. Our standard procedure was to inject [³H]leucine at the beginning of a light period and to maintain the tadpoles on the usual 12L:12D cycle for 24 h until the beginning of the next light period. At this time, a sample of eyes was fixed and the remaining animals were placed under appropriate experimental conditions or maintained on a 12L:12D cycle (controls). During the initial 24-h period after injection, [³H]leucine was incorporated into protein in rod photoreceptors, and a portion of this was transported to the base of the ROS where it appeared as an intense radioactive band (46, 52; see also Fig. 5). Displacement of the radioactive band was measured after this initial 24-h period. Thus, our analysis involved only *displacement of a preformed radioactive band*. The incorporation of [³H]leucine into protein in rod inner segments is a separate problem not considered in the present report.

Calculations of the rate (*R*) of radioactive band (³H-band) displacement were based on the formula

$$R = \frac{Bt_2 - Bt_1}{t_2 - t_1}$$

where *B* is the position of the ³H-band (measured in micrometers from the base of the ROS to the scleral edge of the ³H-band; see Figs. 5–8) and *t* is the elapsed time after injection. In this report, *Bt*₁ was generally the band position after 1 day, and *Bt*₂ was its position at a subsequent time up to 4 days after injection. This provided a consistent means for determining an average rate of ³H-band displacement, taking into account the lag period during the 1st postinjection day during which labeled protein is being incorporated into the ROS.

Preliminary analysis of autoradiographs used in this study indicated the existence of a gradient in ROS dimensions and rate of ^3H -band displacement. ROS in the dorsal retinal field were longer and narrower than those in the central and ventral fields. Paralleling these differences in dimensions were differences in ^3H -band displacement. The ^3H -band tended to be displaced to a greater extent near the dorsal and ventral margin than in the center. When renewed ROS material was considered as volume rather than linear distance to the ^3H -band, the direction of these differences was reversed indicating that despite less ^3H -band displacement, the broader rods near the center of the retina renew their outer segment material more rapidly. Because of these small but consistent differences within a single retina, comparisons among different animals were made only for measurements from the retinal center near the optic nerve where ROS were $5.9 \pm 0.3 \mu\text{m}$ wide (mean \pm standard error) and $23.5 \pm 0.8 \mu\text{m}$ long among animals on a 12L:12D cycle.

For each eye examined, the mean distance from ROS base to the ^3H -band and ROS length were determined on the basis of measurements of at least 10 different longitudinally sectioned ROS. These means were used to calculate the mean and standard error for a particular treatment. In those experiments designed to analyze shedding and ^3H -band displacement simultaneously, phagosome counts were made on the same autoradiographs used for measurements.

Analysis of Phagosomes in the Pigment Epithelium

Our procedure was to count all deeply staining profiles within a $1,000\text{-}\mu\text{m}$ expanse of pigment epithelium (PE) sectioned transversely along the dorsoventral axis of the eye. These structures were heterogeneous in size and shape, and were identified primarily on the basis of their affinity for the cationic dyes. In general, they stained more intensely than the adjacent ROS. On the basis of previous analysis of such structures (4, 24, 51), the deeply staining profiles are referred to as phagosomes throughout this report. Each profile was measured along its greatest dimension and tabulated according to size in bins covering a range of $1.3 \mu\text{m}$ (see Fig. 3). Data are presented either as size frequency histograms based on three animals or as means with standard errors of ranges.

RESULTS

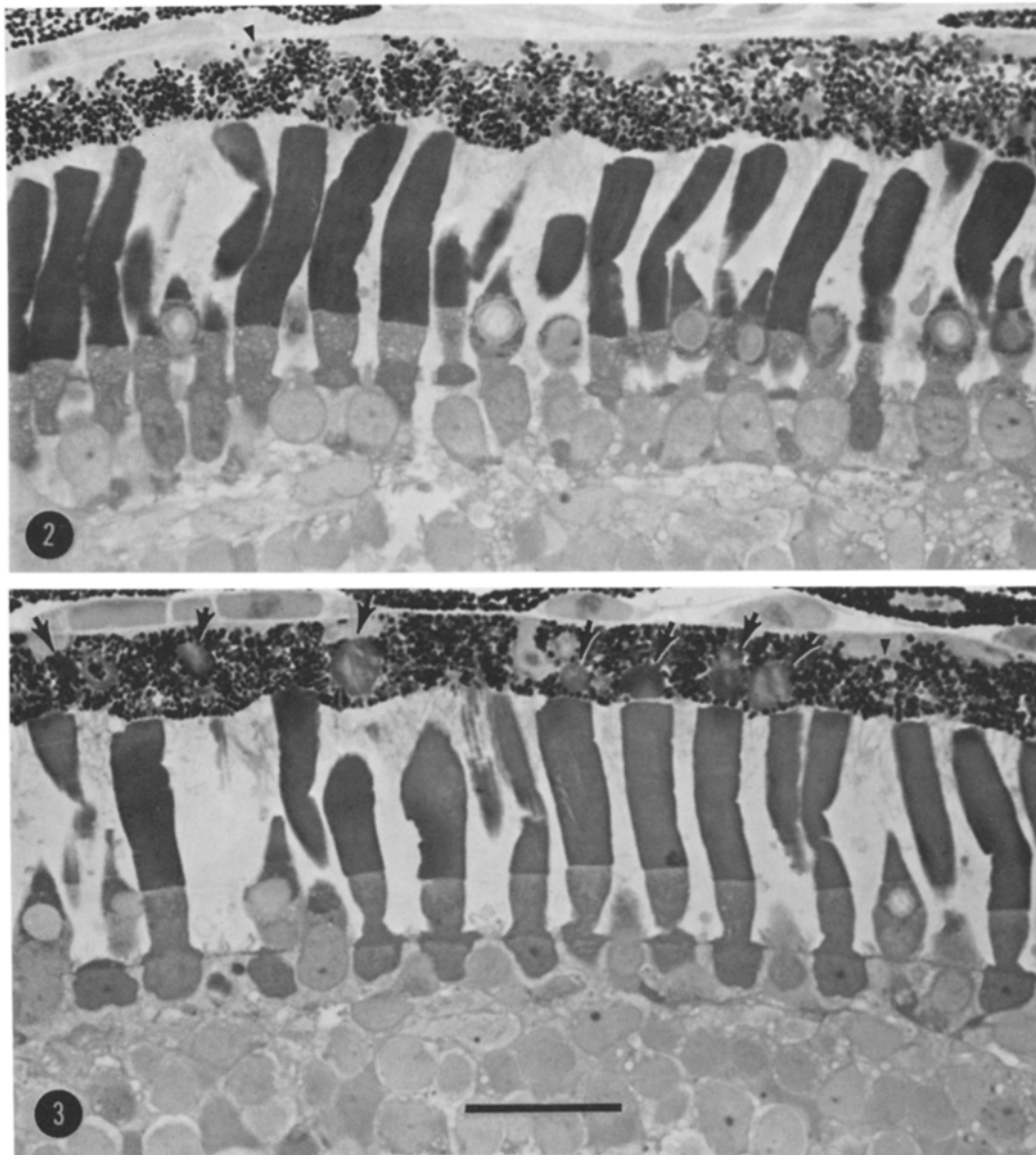
Shedding and ^3H -Band Displacement in Cyclic Light

Shedding by rod photoreceptors of *X. laevis* tadpoles is influenced by cyclic light in the same way as in *Rana pipiens* tadpoles and adults (4, 24, 25). Among animals kept on a 12L:12D

cycle, the number of phagosome profiles in the PE increased dramatically after exposure to light and remained high for about 4 h (Figs. 2 and 3). Thereafter, the phagosome profiles decreased in average size and number, reaching a low level within 24 h (Fig. 4). Previous analyses (4, 24, 25, 51) have established that these phagosome profiles represent the shed tips of ROS, and that monitoring the content of such profiles within the PE provides quantitative information on ROS shedding.

Size frequency distributions of phagosomes within the PE of the eyes fixed throughout the day (Fig. 4) showed that the number of phagosomes $>2 \mu\text{m}$ in size increased after exposure to light and reached a peak within 1 h. This corresponds to one large phagosome for every three ROS visible in the same sections. Small phagosomes ($<2 \mu\text{m}$), however, remained relatively constant in number throughout the day. Thus, during the period from 30 min to 12 h after light exposure, the size frequency distribution was bimodal with a peak at $<2 \mu\text{m}$ and another peak in the $3.3\text{--}4.6 \mu\text{m}$ range. Between 4 and 16 h, there was an approximate doubling of the number of phagosomes in the $2.0\text{--}3.3 \mu\text{m}$ range which may have reflected degradation of larger phagosomes to smaller size. After 12 h, there was a sharp decline in the total number of large phagosomes, with no significant changes in the small-phagosome category.

The rate of disk addition as reflected by ^3H -band displacement also increases immediately after light exposure. 24 h after injection of [^3H]leucine, a ^3H -band was found in ROS an average of $1.5 \pm 0.1 \mu\text{m}$ from the base (Fig. 5). Thereafter, the band was displaced $2.0\text{--}2.5 \mu\text{m}/\text{day}$. The lesser displacement during the first 24 h after injection probably reflected the fact that the [^3H]leucine was initially incorporated into proteins in the inner segment and then transported to the ROS base before incorporation into disks (37, 52). When the ^3H -band position was determined at 8-h intervals over the 24-h period beginning 1 day after injection (Fig. 5), a large proportion of the total displacement was found to occur during the first 8-h period (Figs. 5 and 6), whereas little or no displacement occurred during the final 8 h (Figs. 7 and 8). Measurements from a large number of animals (Fig. 9) indicated that about 75% of the daily increment of ^3H -band displacement occurred during the first 8 h after light exposure. During the period from 8 to 16 h, the



FIGURES 2-3 Light micrographs illustrating photoreceptors and PE of tadpoles kept on a 12L:12D cycle. $\times 1,000$.

FIGURE 2 Preparation from an eye fixed just before the onset of light. The PE is virtually free of large, deeply staining phagosomes. The arrowhead indicates a small phagosome. Same scale as in Fig. 3.

FIGURE 3 Preparation from an eye fixed 4 h after light exposure. Large phagosomes are indicated by the large arrows, and a small phagosome is indicated by the small arrowhead. Bar, 20 μm .

^3H -band advanced somewhat farther. During the last 8 h, however, band displacement was undetectable (Figs. 7, 8, and 9).

These data suggest the possibility that ^3H -band displacement may be a discontinuous process.

Whether the process actually ceases or declines to a low level cannot be determined from these data, however, because continued disk addition at a greatly reduced rate would probably be undetectable over periods as short as 8 h. None-

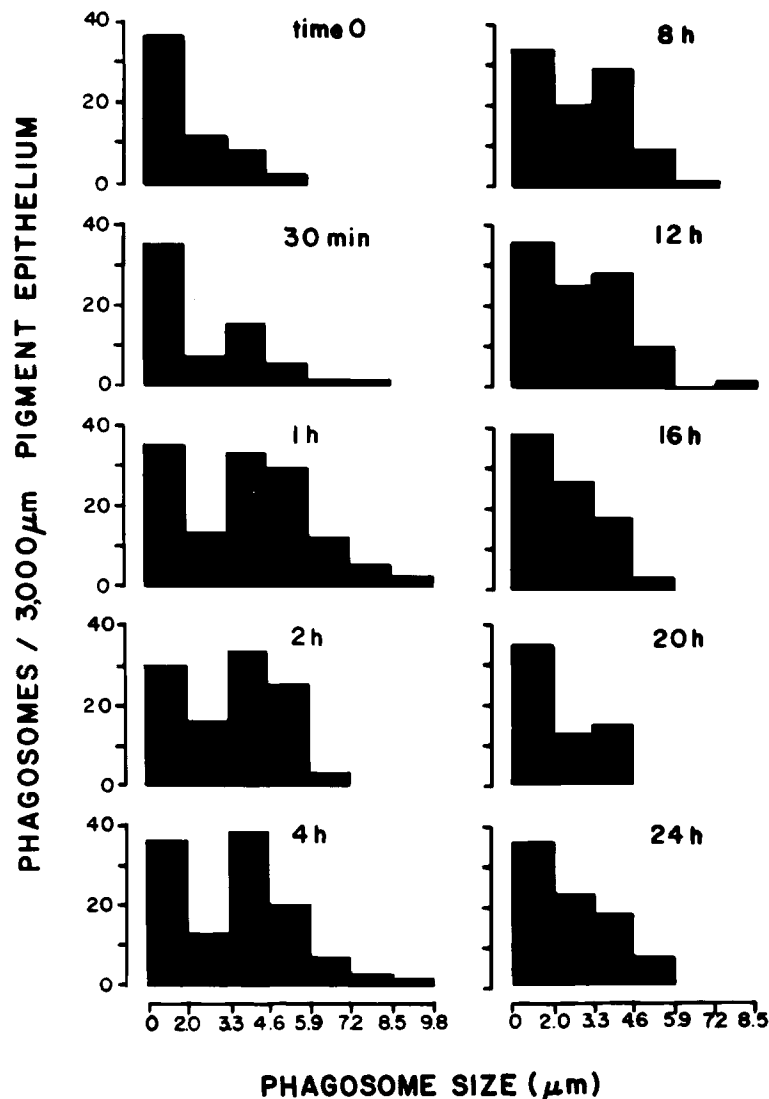
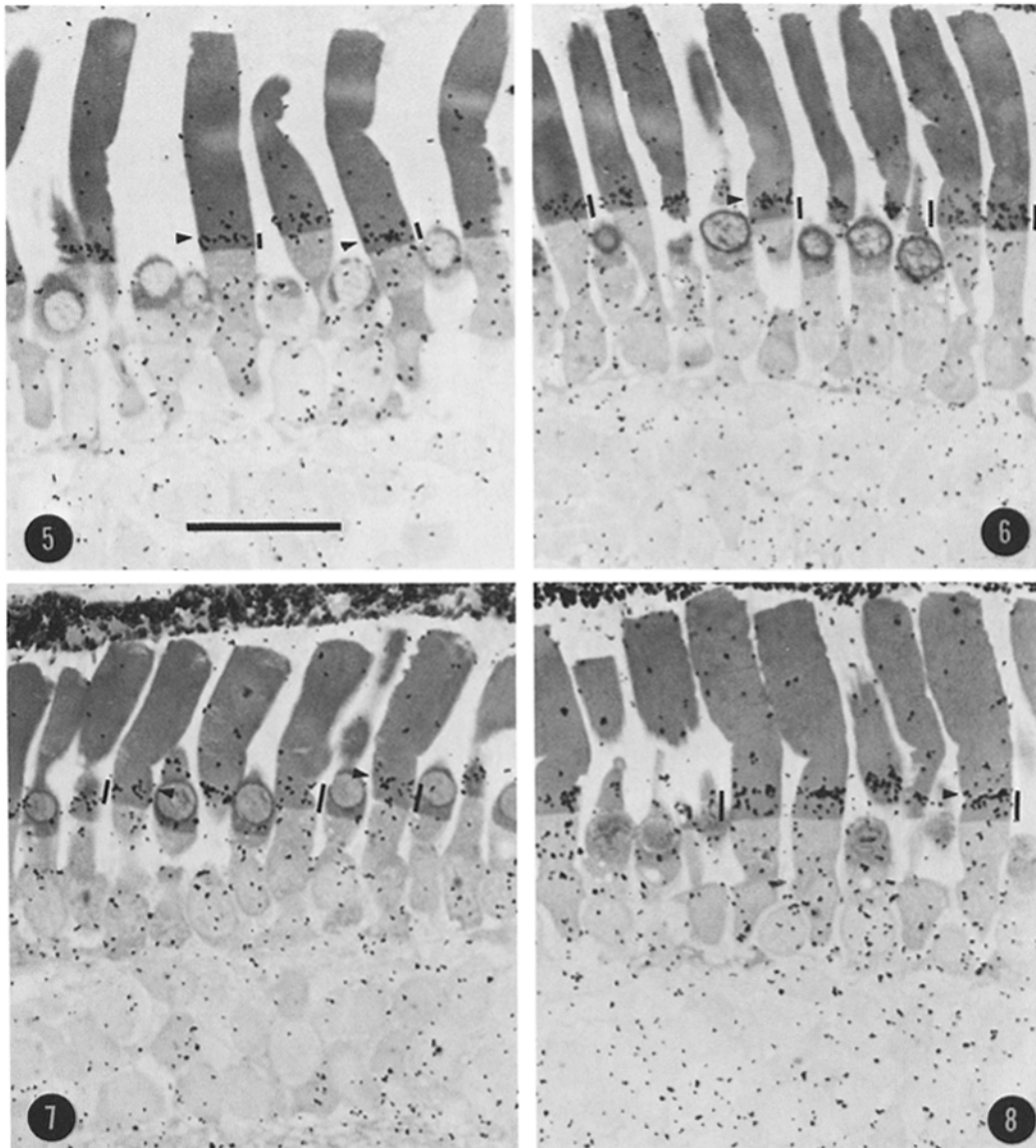


FIGURE 4 Size frequency distributions of phagosomes in the PE of eyes fixed at various times of the day among animals kept on a 12L:12D cycle. Time zero is the beginning of the light period, and 12 h is the beginning of the dark period. Each distribution represents the totals from three animals.

theless, the data clearly indicate that the great majority of disks are normally added early in the day. On the basis of a ^3H -band displacement rate of $2.3 \mu\text{m}/\text{day}$ (Fig. 9) and a mean packing of $36.9 \pm 1.2 \text{ disks}/\mu\text{m}$ of ROS (counts from electron micrographs from eight animals), we estimate that an average of 85 disks are added to the ROS each day. Of these, about 64 must be added during the first 8 h of light. To further study the diurnal differences in disk addition, we used electron microscopy to examine the basal disks of ROS.

Variations in ROS Ultrastructure in Cyclic Light

Previous ultrastructural studies of developing and mature ROS have indicated that disks are added to the base of the ROS in the region immediately adjacent to the connecting cilium (13, 14, 30, 36, 50). In this region, rods typically exhibit a variable number of immature disks which retain continuity with the plasma membrane (14). Our ultrastructural observations indicate that the number of basal disks confluent with the ROS



FIGURES 5-8 Autoradiographs of photoreceptors from eyes fixed at 8-h intervals during the 2nd day after injection of [^3H]leucine. Tadpoles were kept on a 12L:12D cycle and received [^3H]leucine injections at the beginning of the light period 1 day before the fixations. Arrows indicate the scleral edge of the ^3H -bands, and the vertical bars adjacent to the outer segments indicate the distance measured. $\times 1,000$.

FIGURE 5 Photoreceptors fixed at the beginning of the light period (time zero) 1 day after injection of [^3H]leucine. The mean distance to the ^3H -band in a sample of seven animals fixed at the same time was $1.5 \pm 0.08 \mu\text{m}$. Bar, $20 \mu\text{m}$.

FIGURE 6 Photoreceptors fixed 8 h after the onset of light. Note that the distance to the ^3H -band has increased substantially. Scale as in Fig. 5. The mean distance to the ^3H -band in a sample of seven animals fixed at the same time was $3.2 \pm 0.13 \mu\text{m}$.

FIGURE 7 Photoreceptors fixed 16 h after the onset of light. The lights went off 4 h before fixation. Scale as in Fig. 5. The mean distance to the ^3H -band in a sample of seven animals fixed at the same time was $3.6 \pm 0.15 \mu\text{m}$.

FIGURE 8 Photoreceptors fixed 24 h after the onset of light. The lights went off 12 h before fixation. Scale as in Fig. 5. The mean distance to the ^3H -band in a sample of six animals fixed at the same time was $3.8 \pm 0.12 \mu\text{m}$.

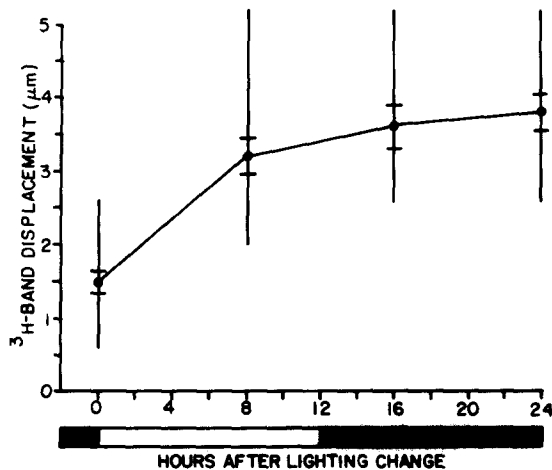


FIGURE 9 Relationship between ^3H -band position in the ROS and time of day during the 2nd day after injection of [^3H]leucine. Points represent means based on six or seven animals. The vertical bars represent the ranges for each sample, and the crossbars mark off a distance equal to two standard errors on both sides of the means.

plasma membrane (open disks) varies in a predictable pattern during a 24-h period.

Open disks of *X. laevis* ROS can be distinguished from mature disks by two criteria. First, at the edge of the ROS the intradiscal space is confluent with the extracellular space (Figs. 10–14). The observation of confluence with the extra-

cellular space cannot be made in all cases, however, because it requires that the plane of section pass through the area of the opening. Second, in longitudinal sections the intradiscal space of open disks is wider than that of closed disks. In our preparations, the intradiscal space of closed disks was very narrow or obliterated altogether, whereas that of open disks varied from 8 to 15 nm across (see Figs. 12, 15, 16). Typical longitudinal sections of ROS revealed a zone of open disks, only some of which were confluent with the extracellular space in the plane of section. In addition, disks of this zone had a greater intradiscal space. Occasionally, a few disks with the structure of closed disks were seen in the open disk zone (Fig. 16). As such disks were identical in structure to closed disks, they were assumed to be closed for purposes of analysis.

Among longitudinally sectioned ROS, the number of open disks was counted in micrographs from eyes fixed throughout the day. Counts were made near the long axis of each ROS profile. The open disks were always confined to a zone no greater than $1\ \mu\text{m}$ in length at the ROS base (Figs. 15 and 16). We counted open disks only in cells having at least one open disk. This decision was made before the analysis and was based on the idea that observation of at least one open disk was necessary to determine unequivocally whether or not the plane of section passed through the

FIGURES 10–14 Electron micrographs illustrating the zone of open disks at the base of the ROS in animals kept on a 12L:12D cycle. Eyes were fixed 4 or 16 h after the onset of light. $\times 60,000$.

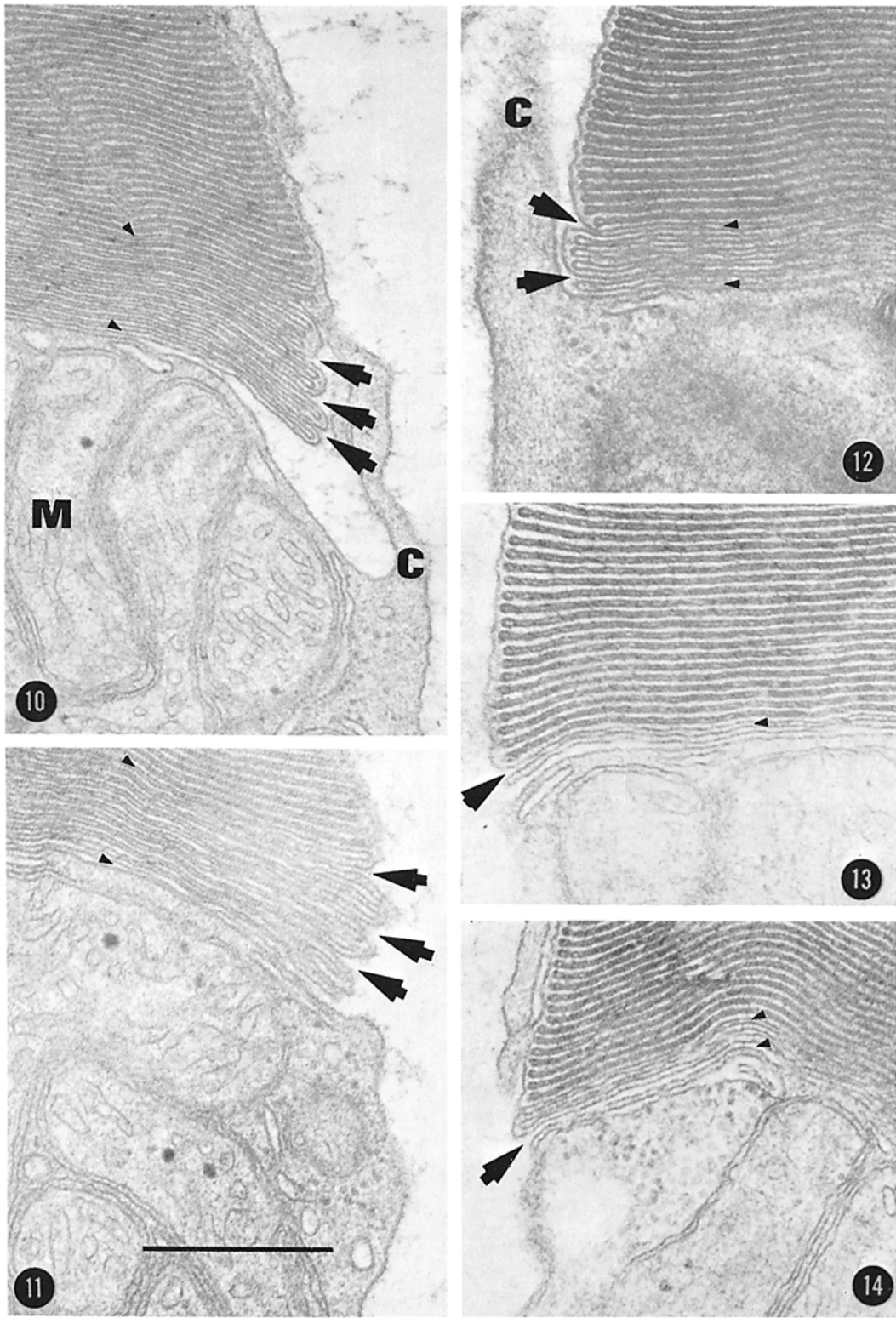
FIGURE 10 Zone of open disks in a ROS fixed 4 h after the onset of light. Note that all the disks in the zone are not open to the extracellular space in the plane of section (large arrows). 12 open disks are present between the two small arrowheads. A calycal process (C) and mitochondrion (M) in the inner segment are labeled. Scale as in Fig. 11.

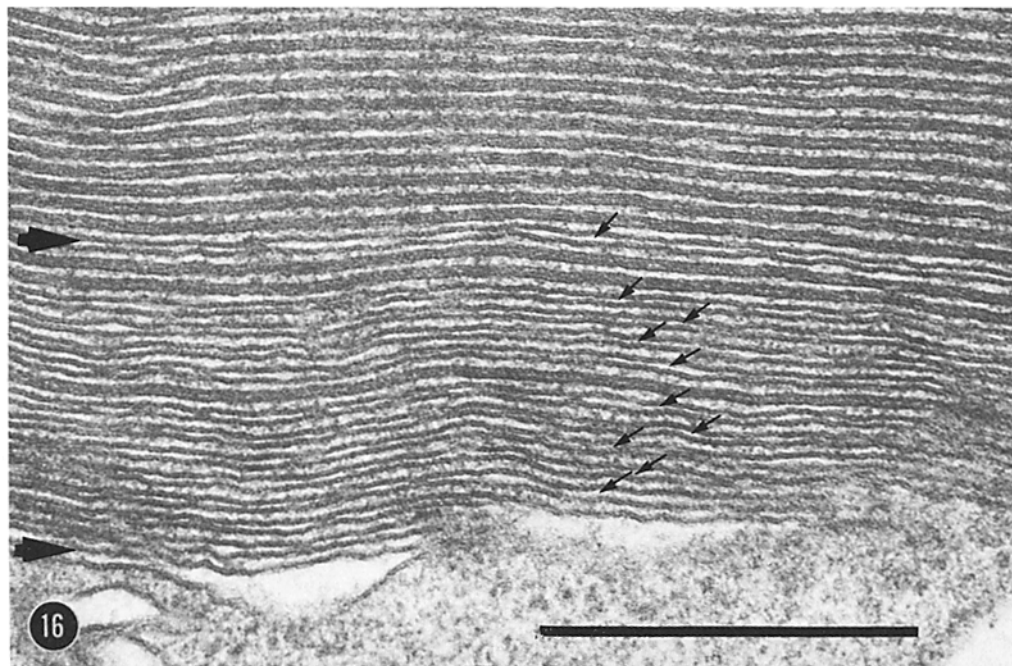
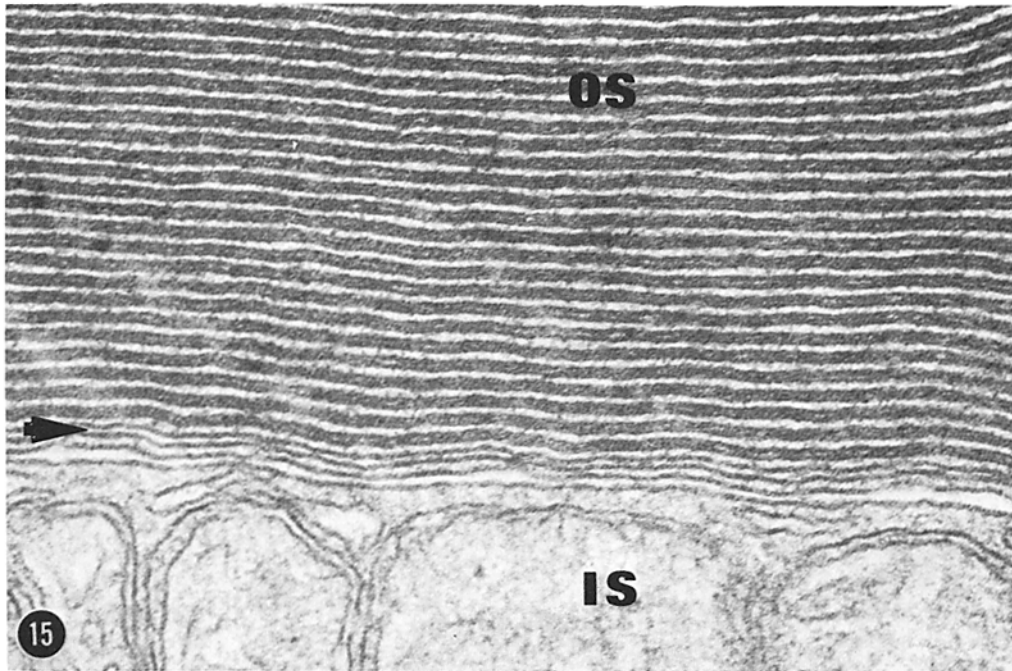
FIGURE 11 Zone of open disks in a ROS fixed 4 h after the onset of light. This preparation is similar to that in Fig. 10. It has 10 open disks between the two small arrowheads. The large arrows indicate points of confluence between the intradiscal space and the extracellular space. Bar, $0.5\ \mu\text{m}$.

FIGURE 12 Zone of open disks in a ROS fixed 4 h after the onset of light. Five open disks are present between the two small arrows. Large arrows indicate points where the intradiscal space is confluent with the extracellular space. Scale as in Fig. 11.

FIGURE 13 Zone of open disks in a ROS fixed 16 h after the onset of light (4 h after the lights went off). Note the presence of a single open disk (small arrowhead) with its intradiscal space confluent with the extracellular space (large arrow). Scale as in Fig. 11.

FIGURE 14 Zone of open disks in a ROS fixed 16 h after the onset of light (4 h after lights went off). This ROS has three open disks (small arrowheads), only one of which shows confluence with the extracellular space (large arrow) in the plane of section. Scale as in Fig. 11.





FIGURES 15-16 Electron micrographs illustrating the zone of open disks at the base of ROS in animals kept on a 12L:12D cycle. Eyes were fixed 4 and 16 h after the onset of light. Large arrows indicate the zone of open disks, and small arrows indicate the intradiscal space. $\times 100,000$.

FIGURE 15 Zone of open disks in a ROS fixed 16 h after the onset of light (4 h after the lights went off). Outer segment (OS) and inner segment (IS) are labeled. A single open disk is present. Scale as in Fig. 16.

FIGURE 16 Zone of open disks in a ROS fixed 4 h after light exposure. 10 open disks are present in the area indicated by small arrows. Three disks with the morphology of closed disks are present in the zone of open disks.

zone of open disks. Subsequent analysis of the data revealed that virtually all ROS except those fixed at 16 h had open disks. Therefore, the mean value reported for eyes fixed at 16 h is probably high (Fig. 17). An average of three open disks was present in darkness and after the 1st h of light exposure (Fig. 17). Within 2 h of light exposure, open disks increased significantly, reaching a peak by 8 h and declining to the nighttime value by 12 h (Fig. 17). Thus, during the period of maximal ^3H -band displacement (Fig. 9), open disks adjacent to the connecting cilium increased more than threefold.

Effects of Modified Lighting Regimes

The observation that both ^3H -band displacement and shedding occur early in the day raises two immediate questions. (a) Does light stimulate one or both processes, or, alternatively, do one or both processes occur as a free-running circadian rhythm for which the external light cycle acts as a cue? (b) Does shedding always accompany accelerated ^3H -band displacement? To obtain data relating to these questions, we analyzed changes in ^3H -band position and shedding in animals maintained under four different lighting regimes (12L:12D, 2.5L:21.5D, constant darkness, and constant light) for 3 days. The object of this

experiment was to simultaneously monitor ^3H -band displacement and phagosome content of the PE. During each 24-h period, eyes from each treatment were fixed at 0, 4, 8, 16, and 24 h after the beginning of the light period in controls (12L:12D). Phagosome content of the PE, ^3H -band displacement, and ROS length were all determined from autoradiographs.

Phagosome profiles $<2\ \mu\text{m}$ in diameter have been shown to be an invariant feature of the frog PE under a variety of experimental conditions (24, 25; see Fig. 4). Likewise, in the present experiment, no significant differences were observed under any of the lighting conditions. The mean number in samples fixed in each lighting condition over the 3-day period ranged from 10.3 ± 1.0 to $11.6 \pm 0.6/1,000\ \mu\text{m}$ of PE. Phagosomes $>2\ \mu\text{m}$ in their greatest dimension, however, varied in a predictable pattern in controls (12L:12D), and this pattern was modified under experimental conditions.

12L:12D (CONTROL): Large phagosome ($>2\ \mu\text{m}$) content of the PE and ^3H -band displacement over 3 days on a 12L:12D cycle are presented in Fig. 18. Mean values ranging from 21 to 28 phagosomes/1,000 μm of PE were found 4 h after light exposure each day. By using the mean number of phagosome profiles at the peaks

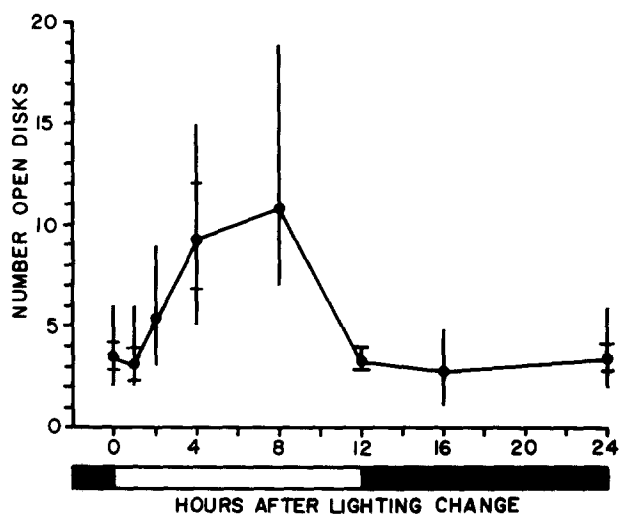


FIGURE 17 Relationship between number of open disks in ROS and time of day among animals kept on a 12L:12D cycle. Points represent means based on two-to-four animals, and vertical bars represent ranges. Crossbars mark off a distance equal to two standard errors on both sides of the means. Standard errors for means based on two animals are not presented. Counts were made on 5-15 ROS per eye (usually at least 10) each having at least one open disk. In the 16-h sample (midnight), many ROS had no open disks.

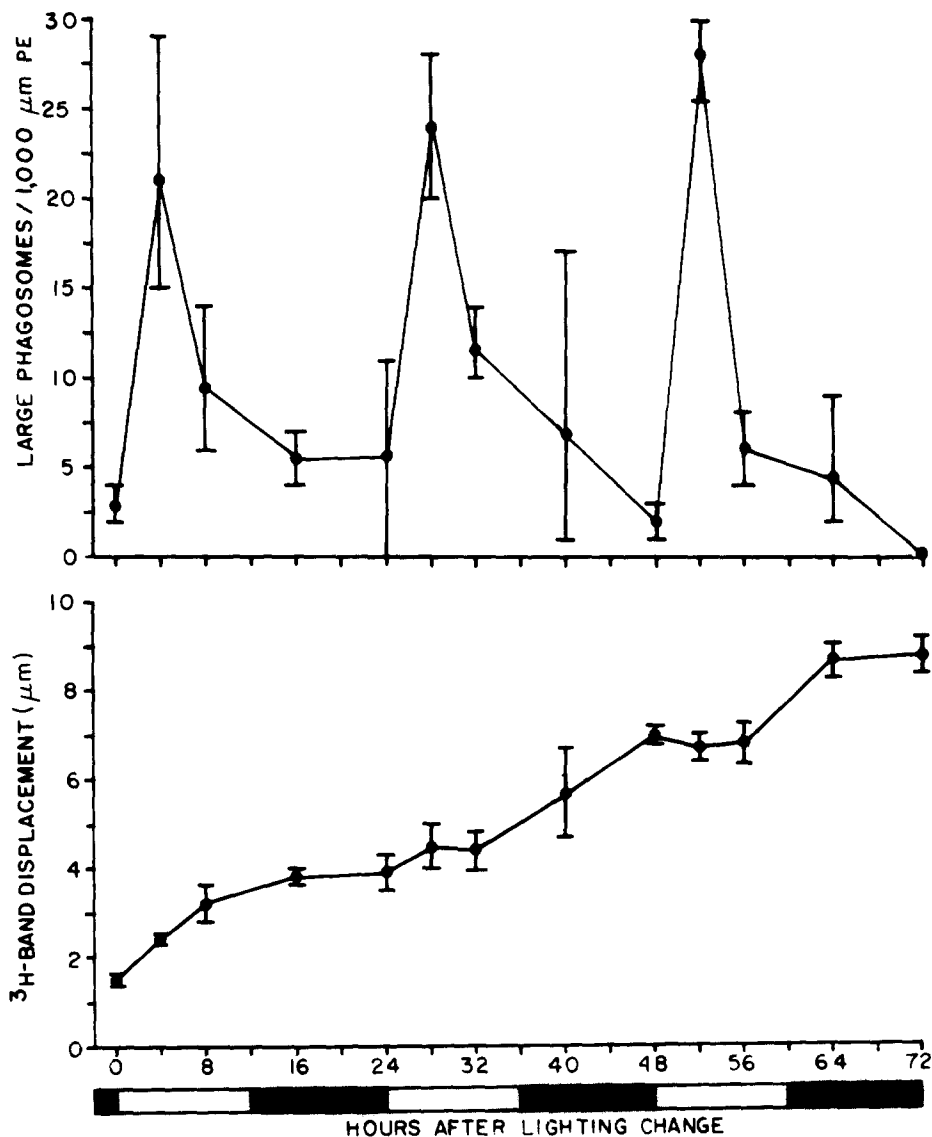


FIGURE 18 Relationships among content of large phagosomes in the PE (above), ³H-band position (below), and time (abscissa) during 3 days on a 12L:12D cycle. This is the control for the experimental data presented in Figs. 22-24. Animals received injections of [³H]leucine 24 h before time zero. Points represent means based on three animals, and vertical bars represent ranges for large phagosomes or two standard errors on both sides of means for ³H-band position. The average rate of ³H-band displacement during the 3-day period was 2.4 μm/day.

(Fig. 18) and assuming that each profile represents the shed tip of a single ROS, we estimate that 22-30% of the ROS shed their tips each day. These estimates are based on the observation that 94.9 ± 1.5 ROS profiles are present along each 1,000-μm expanse of PE. The estimate is probably somewhat low inasmuch as the number of phagosomes found at 4 h is somewhat lower

than at 1 h (cf. Figs. 4 and 18).

During the same 3-day interval, ³H-band displacement occurred at an average rate of 2.4 μm/day (Fig. 18), and during the 1st day (2nd day after injection) was largely confined to the first 8-h interval as reported above (Fig. 9). On the 2nd and 3rd days, however, ³H-band displacement occurred later in the day and did not correspond

to the period of maximal shedding activity. The delay in ^3H -band displacement during the 2nd and 3rd days raises the question of whether or not ^3H -band movement always reflects ongoing disk addition. To examine this, we counted open disks in electron micrographs from selected eyes fixed during the 2nd day of the experiment. The counts were not different from those reported above (Fig. 17), indicating that the temporal pattern of disk addition as reflected in increased numbers of open disks was not modified.

To examine the possibility that the temporal pattern of ^3H -band displacement is related to position of a radioactive band along the longitudinal axis of the ROS, we examined ^3H -band displacement in a group of animals that received two injections of [^3H]leucine 2 days apart. ROS in these animals had two radioactive bands (Fig. 19). The distal band resulted from the first injection,

whereas the proximal band resulted from the second injection. Animals were fixed at 8-h intervals during the 4th day after the first injection. Thus, each ROS contained radioactive bands corresponding to those previously observed on the 1st and 4th postinjection days (Fig. 18). Displacement of each ^3H -band was examined independently.

Both ^3H -bands were displaced just over $2\ \mu\text{m}$ during the 24-h period, but the pattern of displacement differed for each band. Initially, the distal band was $4.8 \pm 0.4\ \mu\text{m}$ from the ROS base and was not displaced significantly during the first 8-h period. In contrast, the proximal band was initially $1.2 \pm 0.2\ \mu\text{m}$ from the base and was displaced approximately 60% of the daily increment during the first 8 h. During the final 8-h period, the distal band was displaced about 55%, whereas significant displacement did not occur

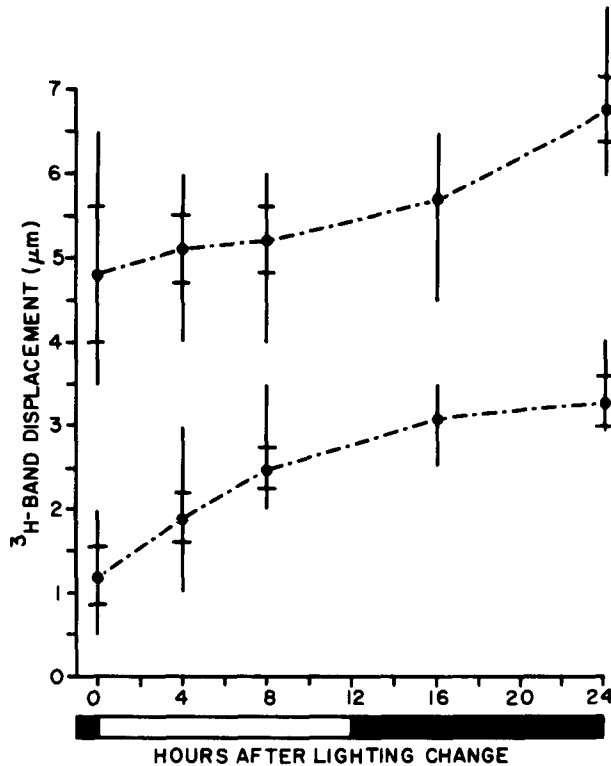


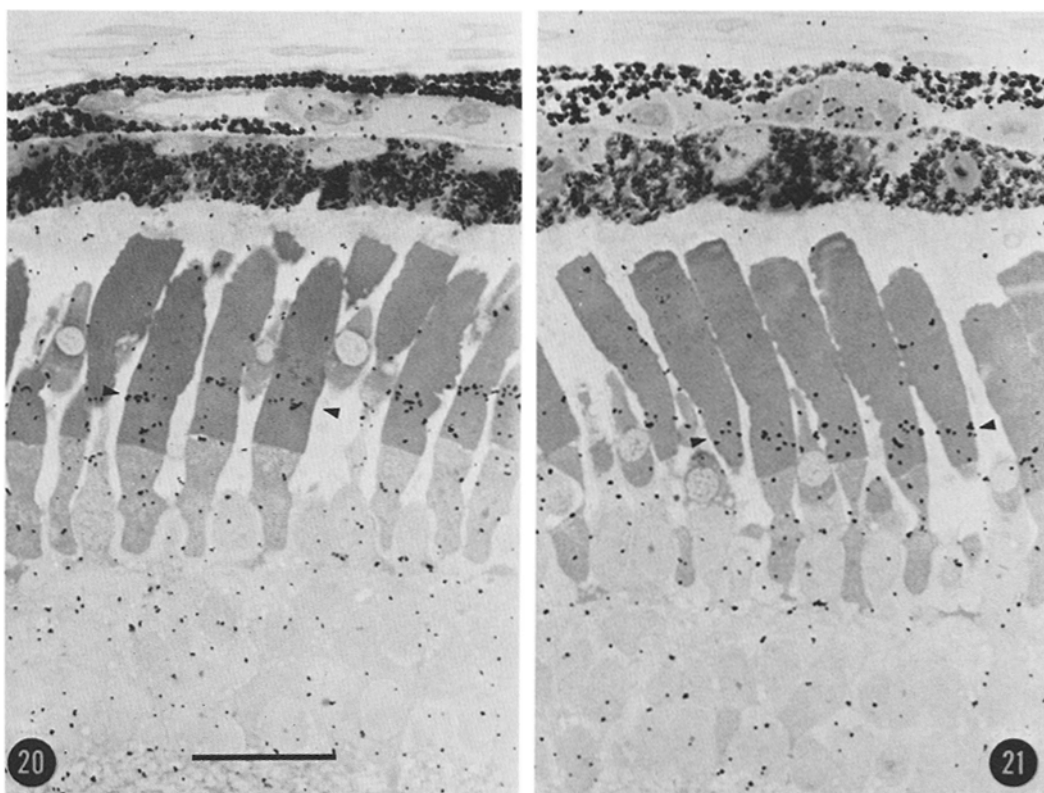
FIGURE 19 Relationship between ^3H -band position in the ROS and time of day in animals given two injections of [^3H]leucine 2 days apart. The upper plot represents the more distal band during the 4th day after the first injection, whereas the lower plot represents the proximal ^3H -band during the same period. Both bands were measured simultaneously in the same sections. Points are means based on one or three animals. Vertical bars represent ranges, and crossbars mark off a distance equal to two standard errors on both sides of the means. The mean at 16 h is based on a single animal, for which the range but not the standard error is given.

for the proximal band. Thus, the proximal band followed a pattern of displacement similar to that previously observed for the 2nd postinjection day (6; Figs. 9 and 18), whereas displacement of the distal band was delayed to the latter part of the day. It appears likely, therefore, that the time of day at which maximal ^3H -band displacement occurs depends on the linear position of the band in the ROS.

CONSTANT DARKNESS: Both ^3H -band displacement and shedding were reduced in darkness (Figs. 20–22). During 3 days of treatment, total ^3H -band displacement averaged 50% of that in controls (Figs. 20 and 21). The average rate of displacement was $1.2 \mu\text{m}/\text{day}$. ^3H -band displace-

ment was slightly higher than this during the first 2 days and was barely detectable on the 3rd day (Fig. 22). The pattern of displacement was that of a gradual trend without periods of distinct acceleration.

Phagosomes in the PE increased in number early each day, but the peak number was found at 8 h rather than at 4 h (Fig. 22). In addition, the total number observed at the peaks was lower than in controls. On the basis of the mean number of phagosomes at the 8-h peaks, we estimate that overall shedding was reduced by about 40% compared to controls. During the first 2 days, shedding was reduced 52–54% whereas on the 3rd day it was comparable to that in controls (Fig. 22).



FIGURES 20–21 Autoradiographs of photoreceptors fixed after 3 days in cyclic light (12L:12D) or darkness. Each animal received an injection of [^3H]leucine 24 h before the beginning of the treatments. Small arrowheads indicate ^3H -bands. $\times 950$.

FIGURE 20 Photoreceptors fixed after 3 days in cyclic light (12L:12D). The mean distance to the ^3H -band in three tadpoles fixed at the same time was $8.8 \pm 0.20 \mu\text{m}$. Bar, $20 \mu\text{m}$.

FIGURE 21 Photoreceptors fixed after 3 days in darkness. The mean distance to the ^3H -band in three tadpoles fixed at the same time was $5.2 \pm 0.13 \mu\text{m}$. This corresponds to a 50% reduction in the rate of ^3H -band displacement calculated over the 3-day treatment period between days 1 and 4 after injection. Scale as in Fig. 20.

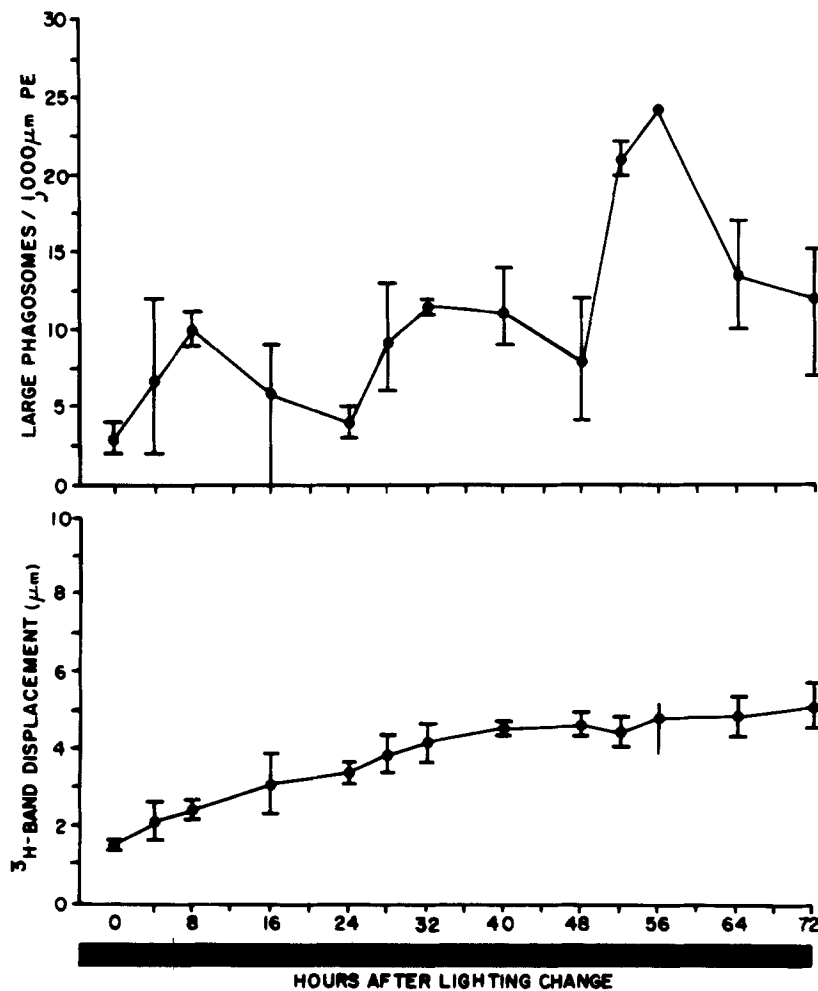


FIGURE 22 Relationships among content of large phagosomes in the PE (above), ^3H -band position (below), and time (abscissa) during 3 days in darkness. Points and vertical bars are as in Fig. 18. The sample at 56 h was based on only two animals, for which a standard error was not calculated. The average rate of ^3H -band displacement was $1.2 \mu\text{m}/\text{day}$.

CONSTANT LIGHT: ^3H -band displacement and shedding were affected differently in constant light (Fig. 23). The average rate of ^3H -band displacement ($2.6 \mu\text{m}/\text{day}$) was not significantly different from that of controls, and during the 1st day of treatment ^3H -band displacement followed a pattern like that of controls. During the 2nd and 3rd days, however, ^3H -band displacement was more irregular and much more variable (cf. Figs. 18 and 23). Because of the increased variability, the suggested discontinuities in ^3H -band displacement during the 2nd and 3rd days (Fig. 23) cannot be regarded as significant. Thus, we cannot determine from available data whether or

not cyclic disk addition in constant light continues after the 1st day.

The same conclusion holds for shedding. The total number of phagosomes in the PE was reduced on each successive day of the experiment (Fig. 23). During the 1st day, which began with a dark to light transition, shedding was comparable to that of controls, whereas during the 2nd and 3rd days there were no clear peaks in shedding. The absence of a peak in shedding activity makes it difficult to estimate the extent of reduction in shedding during the period. However, using the highest mean value during each 24-h period, we estimate that shedding may have been reduced by

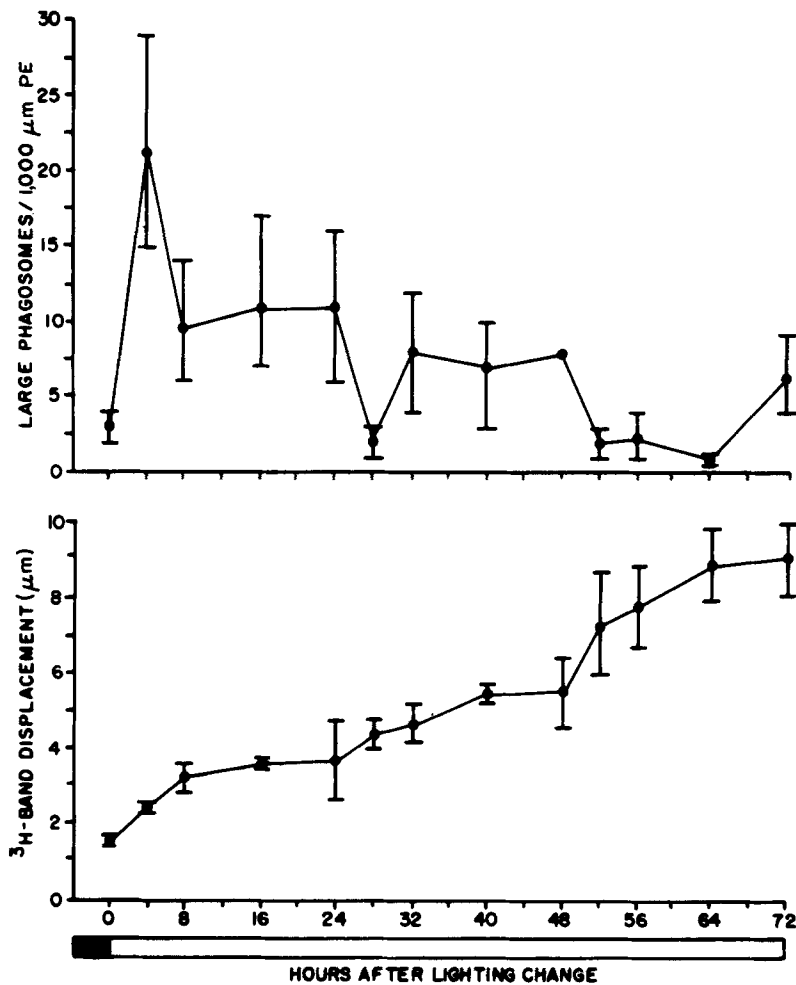


FIGURE 23 Relationships among content of large phagosomes in the PE (above), ³H-band position (below), and time (abscissa) during 3 days in constant light. Points and vertical bars are as in Fig. 18. The average rate of ³H-band displacement was 2.6 μm/day.

70–80%. These values suggest that as few as 6–8% of the ROS shed their tips each day in constant light compared with 22–33% in controls.

2.5L:21.5D: Exposure to 2.5 h of light per day reduced ³H-band displacement substantially, but maintained shedding at near control levels (Fig. 24). Overall, ³H-band displacement was reduced by 38% compared to controls to a level (1.5 μm/day) comparable to that in darkness. The treatment differed from darkness in that the variability, particularly from 40 h onward, was greater. As in darkness and constant light, the data indicate no significant discontinuities in disk addition after the 1st day.

Shedding followed a pattern like that in controls (Fig. 24). The greatest number of phagosomes in

the PE was found 4 h after light exposure each day. The mean number at each peak ranged from 18 to 21. Thus, the level of shedding was reduced by 14–20% compared to controls. The means, however, were well within the range of variation in controls.

Length of ROS

Maintenance of an optimal length of ROS depends on the establishment of a balance between the average rate of disk addition and the average rate of disk loss (31). Treatments that disrupt this balance could lead to either shortening or lengthening of the ROS. During the 3 days of the present experiment, both lengthening and shortening of ROS were observed. During the 1st

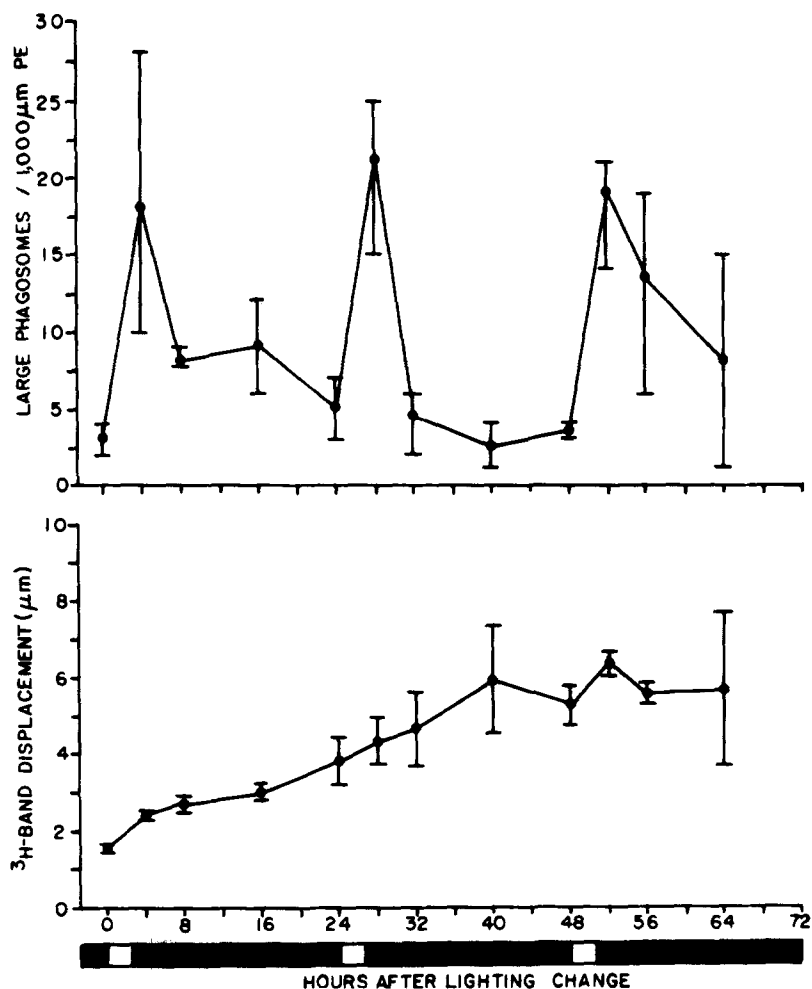


FIGURE 24 Relationships among content of large phagosomes in the PE (above), ³H-band position (below), and time (abscissa) during 3 days on a 2.5L:21.5D cycle. Points and vertical bars are as in Fig. 18. The sample at 72 h was lost before fixation. The average rate of ³H-band displacement was 1.5 μm/day.

day, ROS length was $23.0 \pm 0.5 \mu\text{m}$ for all treatments, with individual samples ranging from 21.3 to 25.0 μm. After 3 days in 12L:12D and darkness, ROS length was, respectively, 24.1 ± 0.9 and $24.4 \pm 0.4 \mu\text{m}$. In constant light where shedding was reduced and disk addition remained high, the mean ROS length after 3 days was $27.7 \pm 0.7 \mu\text{m}$, an increase of 21%. In 2.5L:21.5D where disk addition was reduced to a much greater extent than shedding, ROS length was more variable. In this treatment, after 3 days ROS length was $22.0 \pm 1.9 \mu\text{m}$, a value not significantly different from that of controls at the beginning of the experiment. However, in two of the three animals, ROS ranged from 18 to 19 μm in length,

the shortest length observed in any of the samples of the study. These observations indicate that ROS length increases in constant light and tends to decrease in 2.5L:21.5D.

DISCUSSION

It has been widely assumed that disk addition to ROS and visual pigment biosynthesis occur continuously and are affected by light only slightly. This idea was implicit in the conclusions of Droz (16) whose autoradiographic observations indicated a lack of diurnal variation in protein synthesis by rods of the rat. Although direct evidence was not presented, the idea of continuous activity was later extended to include the processes of

disk addition (46) and visual pigment synthesis and incorporation into ROS membranes (21). In connection with these studies, it was found that light stimulates disk addition slightly (46) and stimulates visual pigment synthesis fourfold (19). It was suggested that the former effect was the result of intraocular heating (48, 50) and that the latter was the result of a modifying action of the PE in darkness (19). Both observations, however, are compatible with our conclusion that *light directly stimulates disk addition to amphibian ROS*.

We have found that levels of illumination normally encountered in nature stimulate ³H-band displacement by 17% in Ozark cave salamanders (5) and by as much as 54% in *R. pipiens* tadpoles and adults (6). To this, we may now add that in *X. laevis* tadpoles ³H-band displacement in cyclic light occurs twice as fast as in darkness. We have also obtained direct evidence that the rate of disk addition to ROS varies widely during a 24-h period and normally occurs as a daily rhythm in cyclic light. During the 2nd day after [³H]leucine injection, the ³H-band in ROS is displaced largely during the first 8 h of light exposure. During this same interval, the number of open disks at the ROS base increases three- to fourfold. In contrast, during the last 8 h in darkness, ³H-band displacement is undetectable and the number of open disks is reduced. These observations together raise the possibility that disk addition may occur discontinuously.

We have also found that the time of ³H-band displacement does not always correspond to the time at which open disks increase in number. In cyclic light, ³H-band displacement during the 3rd and 4th days after injection occurs late in the day, during a time when the number of open disks is reduced. When two ³H-bands resulting from two injections given 2 days apart were analyzed independently during the 4th day after the first injection, we found that they were displaced independently. The band adjacent to the inner segment was, for the most part, displaced early in the day, whereas the more distal band was displaced late in the day. The distance between the two bands decreased between 0 and 8 h and then increased again after 16 h. Inasmuch as there was no evidence of disk loss between the two bands, we interpret these observations as indicating that transient variations in disk packing occurred.

The mechanism of disk displacement in ROS

remains unknown. However, our observations suggest that the ROS is an elastic system in which the force for disk displacement is applied at the base when new disks are formed. Compressive stress in the system may be propagated distally, resulting in transient local variations in disk packing and ³H-band displacement. According to this hypothesis, the time of maximal ³H-band displacement is a function of the time of disk addition (i.e. application of force) and position of the ³H-band along the longitudinal axis of the ROS (i.e. the time at which the force reaches the band). Only when the ³H-band is immediately adjacent to the zone of open disks during the 2nd postinjection day will its displacement reliably reflect the time at which an increase in the number of open disks occurs. Nonetheless, the ³H-band is transported along the ROS at an average rate corresponding to the overall average rate of disk addition.

Our ultrastructural observations on open disks are consistent with the hypothesis that disks form by infolding of the plasma membrane adjacent to the connecting cilium (21, 36, 50). During 8 h in light, the number of open disks increases three- to fourfold. During this same interval, we estimate that as many as 64 disks are added to the ROS. However, this many open disks are never seen at one time. We suggest that all of the open disks formed during this interval do not accumulate because most of them mature and become part of the closed disk system. If it is assumed that the rate of disk maturation (i.e. detachment from the plasma membrane) is constant over the first 8 h, we estimate that closed disk form at the rate of one every 9 min, whereas open disks form at the rate of one every 7.5 min. This rate difference would result in a net accumulation of 11 open disks during the first 8 h of daylight. If the rate of disk maturation remained constant and the rate of open disk formation declined later in the day, the number of open disks would decrease.

How does light accelerate disk addition to ROS? It has been suggested that the small "light effect" in very intense illumination (46) may have been the result of intraocular heating (48, 50). It was reasoned that, because increased temperature itself accelerates ³H-band displacement (46), a local rise in temperature in the microenvironment of the photoreceptors due to light absorption may influence disk addition. Although this explanation appears reasonable for explaining a small "light effect" in levels of illumination exceeding 6,000

1x/m², it is entirely inadequate for explaining the larger "light effects" that we have observed. The temperature increase due to light absorption necessary to account for our observations is simply too large. For example, assuming a temperature coefficient of 2, the doubling of ³H-band displacement in constant light compared to darkness observed in the present report would require a 10°C rise in temperature. This would place the temperature at a level incompatible with cell viability. The same argument pertains to light effects reported in *R. pipiens* tadpoles after exposure to light of short daily duration (6). Thus, even though local temperature variations may occur in the eye, such effects probably play a negligible role in influencing disk addition to ROS.

The fact that shedding of ROS tips occurs predominantly after light exposure (4, 24, 32) during the time when accelerated disk addition begins suggests that the two processes may be directly coupled. This idea is consistent with the observations that in cyclic light an increase in disk addition due to increased temperature is accompanied by a proportional increase in the frequency of ROS shedding (25), and that the frequency of shedding and rate of disk addition are both reduced in darkness. Our observations on animals kept in constant light or on a 2.5L:21.5D cycle, however, indicate that such coupling, if it exists, is very complex. In constant light, a high rate of disk addition is maintained while shedding is dramatically reduced. The result is a rapid increase in ROS length. On the other hand, reduction in the rate of disk addition occurs on a 2.5L:21.5D cycle while shedding is maintained near control levels. These differential effects indicate that a pattern of light alternating with darkness is necessary to sustain normal shedding, whereas light alone is sufficient to maintain normal disk addition. Furthermore, small amounts of light each day are insufficient to maintain the normal disk addition rate. This suggests that light acts as more than a simple trigger in the acceleration of disk addition.

The absence of daily discontinuities in ³H-band displacement in darkness and constant light suggests that the daily rhythm of disk addition observed in cyclic light is abolished under these conditions. We conclude, therefore, that light stimulation plays a predominant role in establishing rhythmicity in cyclic light. In contrast, our observations on shedding of large phagosomes suggest the existence of an underlying endogenous

rhythm. Although delayed in comparison to animals kept on a 12L:12D cycle, a peak in the phagosome content of the PE is found early in each 24-h period. In addition, the mean number of phagosomes at the peak increases from a very low level on the 1st day to a level comparable to that occurring in cyclic light on the 3rd day. The increased number of phagosomes on the 3rd day is similar to the increase previously observed in *R. pipiens* tadpoles kept in darkness (24), and may be related to the decreased rate of disk addition during the same interval. Possibly, the addition of fewer disks to the ROS each day in darkness results in each ROS attaining a size sufficient for shedding later than normal. The observed delay in the peak of large phagosomes in darkness could result from a drift of the endogenous rhythm to a period longer than 24 h as often occurs for free-running rhythms in the absence of external cues (12). Alternatively, it could simply result from protracted shedding in the absence of a light stimulus to synchronize the process.

In rats, shedding occurs as a circadian rhythm in which the number of phagosomes increases early each day in darkness (32). In contrast, it has been suggested that shedding in adult *R. pipiens* normally requires light (4). Because the pattern of shedding in darkness was not determined in the latter experiments, the question of circadian rhythmicity remains open for adult frogs. It appears that the number of phagosomes produced in darkness is reduced in rats because it is known that ROS increase in length in darkness¹ and that the number of phagosomes actually observed early in the day (after the 1st day) is lower than in cyclic light (32). It is not known, however, whether the peak in phagosome content of the PE is delayed because counts at intermediate time points were not made. In general, observations on *X. laevis* and *R. pipiens* (24, 25) tadpoles in darkness are in accord with those on rats (32). The available data for rats and frogs are consistent with the idea that there is an endogenous circadian rhythm of shedding, and that light exposure, in addition to acting as an external cue, also increases the level of shedding above that observed in darkness.

Rodent photoreceptors may differ from amphibians photoreceptors. We have found that there are no significant differences in the rate of

¹ La Vail, M. M. Personal communication.

³H-band displacement among pigmented mice kept in cyclic light, darkness, or constant light for 3 days. Electron microscope observations of open disks, however, suggest that disk addition occurs largely in daylight.² These observations suggest that both shedding and disk addition occur as circadian rhythms which are entrained to an external light cycle.

At the present time, we do not know how cyclic light influences shedding. In addition to stimulating photoreceptors directly, it may influence the eye through its effects on serotonin-melatonin metabolism (32). This idea is consistent with the observed rhythmicity in darkness and the lack of rhythmicity in constant light. Pineal gland and blood concentrations of melatonin occur as free-running rhythms in darkness which are abolished in constant light (29). Furthermore, reserpine, a drug known to abolish some circadian rhythms through its effects on the pineal gland, reduces shedding in the rat (32). If this hormonal system does affect shedding in amphibia, however, the control processes are likely to be complicated because the eye is a major site of serotonin-melatonin metabolism (2), and pinealectomy does not reduce shedding (15).

This work was supported by National Institutes of Health research grants EY 00624, EY 01632, Research Career Development Award EY 00023, National Research Service Award EY 05119, and by a grant from Fight for Sight, Inc.

Received for publication 25 April 1977, and in revised form 21 July 1977.

REFERENCES

1. BAIRATI, A., JR., and N. ORZALESI. 1963. The ultrastructure of the pigment epithelium and of the photoreceptor-pigment epithelium junction in the human retina. *J. Ultrastruct. Res.* **9**:484-496.
2. BAKER, P. C., W. B. QUAY, and J. AXELROD. 1965. Development of hydroxyindole-*O*-methyl transferase activity in eye and brain of the amphibian, *Xenopus laevis*. *Life Sci.* **4**:1981-1987.
3. BASINGER, S., D. BOK, and M. HALL. 1976. Rhodopsin in the rod outer segment plasma membrane. *J. Cell Biol.* **69**:29-42.
4. BASINGER, S., R. HOFFMAN, and M. MATTHES. 1976. Photoreceptor shedding is initiated by light in the frog retina. *Science (Wash. D.C.)*. **194**:1074-1076.
5. BESHARSE, J. C., and J. G. HOLLYFIELD. 1976. Renewal of normal and degenerating photoreceptor outer segments in the Ozark cave salamander. *J. Exp. Zool.* **198**:287-302.
6. BESHARSE, J. C., J. G. HOLLYFIELD, and M. E. RAYBORN. 1977. Photoreceptor outer segments: accelerated membrane renewal in rods after exposure to light. *Science (Wash. D. C.)*. **196**:536-538.
7. BLAUROCK, A. E., and M. H. F. WILKINS. 1969. Structure of frog photoreceptor membranes. *Nature (Lond.)*. **223**:906-909.
8. BOROVJAGIN, V. L., and T. A. IVANINA. 1973. An ultrastructural study of the frog retinal rod photoreceptor membranes phagocytosed by pigment epithelium cells after aldehyde fixations and organic solvents treatments. *Vision Res.* **13**:753-757.
9. BOWNS, D., A. GORDON-WALKER, A. C. GUIDE-HUGUENIN, and W. ROBINSON. 1971. Characterization and analysis of frog photoreceptor membranes. *J. Gen. Physiol.* **58**:225-237.
10. BRIDGES, C. D. B. 1972. The rhodopsin-porphyrin visual system. In *Handbook of Sensory Physiology*. H. J. A. Dartnall, editor. Springer-Verlag, Berlin. 417-480.
11. BRIDGES, C. D. B., J. G. HOLLYFIELD, J. C. BESHARSE, and M. E. RAYBORN. 1976. Visual pigment loss after light-induced shedding of rod outer segments. *Exp. Eye Res.* **23**:637-641.
12. BROWN, F. A., JR. 1973. Biological rhythms. In *Comparative Animal Physiology*. W. B. Saunders Co., Philadelphia. 429-456.
13. COHEN, A. I. 1968. New evidence supporting the linkage to extracellular space of outer segment saccules of frog cones but not rods. *J. Cell Biol.* **37**:424-444.
14. COHEN, A. I. 1970. Further studies on the question of the patency of saccules in outer segments of vertebrate photoreceptors. *Vision Res.* **10**:445-453.
15. CURRIE, J., and J. G. HOLLYFIELD. 1977. Darkness is required for shedding of frog rods. Presented at the Association for Research in Vision and Ophthalmology Meeting, Sarasota, Fla., April 1977.
16. DROZ, B. 1963. Dynamic condition of proteins in the visual cells of rats and mice as shown by radioautography with labeled amino acids. *Anat. Rec.* **145**:157-167.
17. DROZ, B., A. RAMBOURG, and L. OLIVIER. 1963. Action de la lumière sur l'incorporation de méthionine ³⁵S au niveau de la rétine de la Souris. *C. R. Seances Soc. Biol. Fl.* **157**:2136-2140.
18. HAGINS, W. A. 1972. The visual process: excitatory mechanisms in the primary receptor cells. *Annu. Rev. Biophys. Bioeng.* **1**:131-158.
19. HALL, M. O., and D. BOK. 1974. Incorporation of (³H) vitamin A into rhodopsin in light- and dark-adapted frogs. *Exp. Eye Res.* **18**:105-117.
20. HALL, M. O., D. BOK, and A. D. E. BACHARACH. 1968. Visual pigment renewal in the mature frog retina. *Science (Wash. D. C.)*. **161**:787-789.

² Besharse, J. C., and J. G. Hollyfield. Effects of light on disk addition to rod photoreceptor outer segments of the mouse. Manuscript in preparation.

21. HALL, M. O., D. BOK, and A. D. E. BACHARACH. 1969. Biosynthesis and assembly of the rod outer segment membrane system: formation and fate of visual pigment in the frog retina. *J. Mol. Biol.* **45**:397-406.
22. HAMBURGER, V. 1960. A Manual of Experimental Embryology. The University of Chicago Press, Chicago. 221.
23. HELLER, J. 1968. Structure of visual pigments. I. Purification, molecular weight and composition of bovine visual pigment₅₀₀. *Biochemistry* **7**:2906-2913.
24. HOLLYFIELD, J. G., J. C. BESHARSE, and M. E. RAYBORN. 1976. The effect of light on the quantity of phagosomes in the pigment epithelium. *Exp. Eye Res.* **23**:623-635.
25. HOLLYFIELD, J. G., J. C. BESHARSE, and M. E. RAYBORN. Turnover of rod photoreceptor outer segments: membrane addition and loss in relationship to temperature. *J. Cell Biol.* **75**:490-506.
26. ISHIKAWA, T., and E. YAMADA. 1970. The degradation of the photoreceptor outer segment within the pigment epithelial cell of rat retina. *J. Electron Microsc.* **19**:85-91.
27. JAN, L. Y., and J.-P. REVEL. 1974. Ultrastructural localization of rhodopsin in the vertebrate retina. *J. Cell Biol.* **62**:257-273.
28. JOHNSON, N. F. 1975. Phagocytosis in the normal and ischaemic retinal pigment epithelium of the rabbit. *Exp. Eye Res.* **20**:97-107.
29. KLEIN, D. C. 1974. Circadian rhythms in indole metabolism in the rat pineal gland. In *The Neurosciences Third Study Program*. F. O. Schmitt and F. G. Worden, editors. The M.I.T. Press, Cambridge, Mass. 509-515.
30. LATIES, A. M., D. BOK, and P. LIEBMAN. 1976. Procion yellow: a marker dye for outer segment disc patency and for rod renewal. *Exp. Eye Res.* **23**:139-148.
31. LAVAIL, M. M. 1973. Kinetics of rod outer segment renewal in the developing mouse retina. *J. Cell Biol.* **58**:650-661.
32. LAVAIL, M. M. 1976. Rod outer segment disc shedding in rat retina: relationship to cyclic lighting. *Science (Wash. D. C.)*. **194**:1071-1074.
33. LAVAIL, M. M. 1976. Rod outer segment disc shedding in relation to cyclic lighting. *Exp. Eye Res.* **23**:277-280.
34. LIEBMAN, P. A., and G. ENTINE. 1974. Lateral diffusion of visual pigment in photoreceptor disc membranes. *Science (Wash. D. C.)*. **185**:457-459.
35. NIEUWKOOP, P. D., and J. FABER. 1967. Normal Table of *Xenopus laevis* (Daudin). North-Holland Publishing Co., Amsterdam. 245.
36. NILSSON, S. E. G. 1964. Receptor cell outer segment development and ultrastructure of the disc membranes in the retina of the tadpole (*Rana pipiens*). *J. Ultrastruct. Res.* **11**:581-621.
37. PAPERMASTER, D. S., C. A. CONVERSE, and M. ZORN. 1976. Biosynthetic and immunochemical characterization of a large protein in frog and cattle rod outer segment membranes. *Exp. Eye Res.* **23**:105-115.
38. POO, M.-M., and R. A. CONE. 1973. Lateral diffusion of rhodopsin in *Necturus* rods. *Exp. Eye Res.* **17**:503-510.
39. RIPPS, H., M. SHAKIB, and E. D. MACDONALD. 1976. Peroxidase uptake by photoreceptor terminals of the skate retina. *J. Cell Biol.* **70**:86-96.
40. SCHACHER, S., E. HOLTZMAN, and D. C. HOOD. 1976. Synaptic activity of frog retinal photoreceptors; a peroxidase uptake study. *J. Cell Biol.* **70**:178-192.
41. SJÖSTRAND, F. S. 1961. Electron microscopy of the retina. In *The Structure of the Eye*. Academic Press, Inc., New York. 1-28.
42. SPITZNAS, M., and M. J. HOGAN. 1970. Outer segments of photoreceptors and the retinal pigment epithelium. *Arch. Ophthalmol.* **84**:810-819.
43. TOMITA, T. 1970. Electrical activity of vertebrate photoreceptors. *Q. Rev. Biophys.* **3**:179-222.
44. WALD, G. 1968. Molecular basis of visual excitation. *Science (Wash. D. C.)*. **162**:230-239.
45. WORTHINGTON, C. R. 1971. Structure of photoreceptor membranes. *Fed. Proc.* **30**:57-63.
46. YOUNG, R. W. 1967. The renewal of photoreceptor outer segments. *J. Cell Biol.* **33**:61-72.
47. YOUNG, R. W. 1968. Passage of newly formed protein through the connecting cilium of retinal rods in the frog. *J. Ultrastruct. Res.* **23**:462-473.
48. YOUNG, R. W. 1969. The organization of vertebrate photoreceptor cells. In *The Retina*. B. R. Straatsma, M. O. Hall, R. A. Allen, and F. Crescibelli, editors. University of California Press, Berkeley. 177-210.
49. YOUNG, R. W. 1971. The renewal of rod and cone outer segments in the rhesus monkey. *J. Cell Biol.* **49**:303-318.
50. YOUNG, R. W. 1976. Visual cells and the concept of renewal. *Invest. Ophthalmol.* **15**:700-725.
51. YOUNG, R. W., and D. BOK. 1969. Participation of the retinal pigment epithelium in the rod outer segment renewal process. *J. Cell Biol.* **42**:392-403.
52. YOUNG, R. W., and B. DROZ. 1968. The renewal of protein in retinal rods and cones. *J. Cell Biol.* **39**:169-184.